This is a preprint, the final version is subject to change, of the American Mineralogist (MSA)
Cite as Authors (Year) Title. American Mineralogist, in press.
(DOI will not work until issue is live.) DOI: http://dx.doi.org/10.2138/am-2017-6153

Single crystal synthesis of δ-(Al,Fe)OOH

Takaaki Kawazoe[1*], Itaru Ohira[2], Takayuki Ishii[1], Tiziana Boffa Ballaran[1],
Catherine McCammon[1], Akio Suzuki[2] and Eiji Ohtani[2,3]

[1]Bayerisches Geoinstitut, University of Bayreuth, 95440 Bayreuth, Germany

[2]Department of Earth Sciences, Tohoku University, Sendai, Miyagi 980-0845, Japan.

[3]V.S. Sobolev Institute of Geology and Mineralogy, SB RAS, 630090 Novosibirsk, Russia

ABSTRACT

Single crystals of δ-AlOOH, δ-($Al_{0.953}$,$Fe_{0.047}$)OOH and δ-($Al_{0.878}$,$Fe_{0.122}$)OOH with dimensions up to ~0.4-0.6 mm were synthesized by the high-pressure hydrothermal method. Synthesis experiments were performed at 21 GPa and 1470 K for 4 h using a Kawai-type multi-anvil apparatus. The crystals of δ-AlOOH, δ-($Al_{0.953}$,$Fe_{0.047}$)OOH and δ-($Al_{0.878}$,$Fe_{0.122}$)OOH were colorless, yellowish green and brown, respectively. Mössbauer spectra showed 95-100% $Fe^{3+}/\Sigma Fe$ at the octahedral site in δ-(Al,Fe)OOH. Chemical compositions of δ-($Al_{0.953}$,$Fe_{0.047}$)OOH and δ-($Al_{0.878}$,$Fe_{0.122}$)OOH are homogeneous with

Fe/(Al+Fe) of 0.0469(8) and 0.122(3), respectively. Unit-cell parameters of δ-AlOOH are consistent with those of previous studies, and they increase with Fe/(Al+Fe). These results confirm that δ-AlOOH can form a solid solution with ε-FeOOH. The crystals contained a small number of fluid inclusions. The syntheses of large single crystals of δ-(Al,Fe)OOH will facilitate investigation of their phase stability, physical properties including elasticity and elastic anisotropy, behavior of hydrogen bonding and spin state of Fe, which will improve models of the water and oxygen cycles in the deep Earth.

Keywords: δ-AlOOH, δ-(Al,Fe)OOH, water, single crystal, hydrous mineral, high-pressure synthesis, Kawai-type multianvil apparatus

INTRODUCTION

δ-AlOOH is an important phase in the deep water cycle because: (1) a large amount of water can be incorporated in its crystal structure; (2) this phase is stable in hydrous pyrolite mantle (Ohtani et al., 2001), hydrous basalt (Suzuki et al., 2000) and hydrous sediment components (Rapp et al., 2008) of slabs descending into the mantle transition zone (MTZ) and lower mantle; (3) this phase can carry water to the core-mantle boundary (Ohira et al., 2014;

Sano et al., 2008); (4) chemical reaction between δ-AlOOH and Fe-Ni alloy can deliver hydrogen to the Earth's core (Terasaki et al., 2012). Consequently, the physical and chemical properties of δ-AlOOH are of fundamental importance to understanding the water cycle in the MTZ, the lower mantle and the core.

Previous single-crystal X-ray diffraction (SC-XRD) studies of δ-AlOOH and δ-$(Al_{0.84},Mg_{0.07},Si_{0.09})$OOH include crystal structure refinements (Komatsu et al., 2006; Kudoh et al., 2004) and pressure-induced phase transitions (Kuribayashi et al., 2014). The dimensions of crystals were less than 83 μm in the mentioned studies, however. While such sizes are sufficient for structure determinations, larger crystals (> 100 μm) of high quality are required for measurements of physical and chemical properties, for example as prepared by the focused ion beam technique to obtain specific dimensions, shapes and crystallographic orientations (Marquardt and Marquardt, 2012).

The effect of Fe substitution on the physical and chemical properties of δ-AlOOH has not yet been studied. Fe is expected to be accommodated in δ-AlOOH as Fe^{3+} in the MTZ and the lower mantle because ε-Fe^{3+}OOH is isostructural with δ-AlOOH (Chenavas et al., 1973) and stable above 6 GPa at high temperature (Gleason et al., 2008; Nishihara and Matsukage, 2016).

Fe-bearing δ-AlOOH might exist in descending slabs and therefore carry Fe^{3+} (oxygen) into the deep Earth.

In this study, we synthesized single crystals of δ-AlOOH, δ-$(Al_{0.953},Fe_{0.047})$OOH and δ-$(Al_{0.878},Fe_{0.122})$OOH with dimensions up to ~0.4-0.6 mm using a high-pressure hydrothermal method. We report results of sample characterization that includes evaluation of crystal quality, the presence of inclusions, chemical composition and unit-cell parameters. We discuss implications for the stability of δ-(Al,Fe)OOH and the water and oxygen cycles in the MTZ and the lower mantle.

EXPERIMENTAL METHODS

Synthesis experiments

Starting materials were either reagent grade $Al(OH)_3$ powder or mixtures of reagent grade $Al(OH)_3$ and Fe_2O_3 powders with Fe/(Al+Fe) = 0.06 or 0.15 in molar ratios. The Fe_2O_3 powder contained 96.64% $^{57}Fe_2O_3$. The mixtures of $Al(OH)_3$ and ^{57}Fe-enriched Fe_2O_3 powders were ground in an agate mortar with acetone for 1 h. The starting material was packed into a $Au_{80}Pd_{20}$ capsule with inner and outer diameters of 0.9 and 1.2 mm, respectively. The lengths

the capsules for the syntheses of Fe-free and Fe-bearing δ-AlOOH were 3.3 and 2.0 mm, respectively. The capsules were closed by welding.

Synthesis experiments were conducted at 21 GPa using a Kawai-type multi-anvil apparatus with split-sphere type guide blocks (Keppler and Frost, 2005; Rubie, 1999). The capsule was loaded into a Cr-doped MgO octahedron with a 10-mm edge length. We used second-stage anvils made of tungsten carbide (ha-7%, hawedia) with 4-mm truncation and pyrophyllite gaskets with a 3.0-mm width. The sample was heated using a $LaCrO_3$ furnace with inner and outer diameters of 1.8 and 2.5 mm, respectively, surrounded by a ZrO_2 thermal insulator with 0.65-mm thickness. The ceramic parts of the cell assembly were fired at 1273 K before assembling them into the final configuration. Sample pressure was calibrated as a function of press load using phase transformations between forsterite and wadsleyite in Mg_2SiO_4 at 1673 K (Morishima et al., 1994) and between wadsleyite and ringwoodite in Mg_2SiO_4 at 1873 K (Suzuki et al., 2000).

The sample was first compressed at room temperature to a press load of 570 tons. Temperature was then increased to 1470 K at a rate of 40-50 K/min, and the target temperature was held constant for 4 h before rapid quenching. We estimated temperature based on the

84 temperature-power relation obtained in separate runs. The uncertainty in temperature is estimated
85 to be ±50 K. The sample was decompressed to ambient pressure at room temperature over 13 h.
86
87 **Sample analyses**
88 Crystals were selected based on the absence of twinning using a polarizing microscope
89 (Leitz, Laborlux 12 Pol S) and on the quality of their diffraction profiles (full width at half
90 maximum of omega scans <0.1°). Unit-cell lattice parameters were obtained from the vector
91 least-squares fit (Ralph and Finger, 1982) of 23-28 reflections centered following the 8-position
92 centering method (King and Finger, 1979) using a Huber four-circles diffractometer with Mo Kα
93 radiation operated at 50 kV and 40 mA, which were equipped with a point detector and driven by
94 the SINGLE software (Angel and Finger, 2011).
95 The chemical compositions of the Fe-bearing crystals were measured using an electron
96 microprobe operating in wavelength-dispersive mode (JEOL, JXA-8800 installed at Tohoku
97 University) operated at 15 kV and 10 nA. Mössbauer spectra were collected on several crystals
98 with dimensions of ~0.1-0.2 mm at room temperature in transmission mode using a constant
99 acceleration Mössbauer spectrometer with a ^{57}Co source. We collected Mössbauer spectra for 1
100 day and fitted them using Lorentzian doublets assigned to octahedral Fe^{3+} and Fe^{2+} using the

101 program MossA (Prescher et al., 2012). The abundance of Fe^{3+} and Fe^{2+} and their uncertainties
102 were determined from relative areas and statistical fitting errors, respectively.
103

104 **RESULTS AND DISCUSSION**

105 Single crystals of δ-AlOOH, δ-$(Al_{0.953},Fe_{0.047})$OOH and δ-$(Al_{0.878},Fe_{0.122})$OOH with
106 dimensions up to ~0.4-0.6 mm were successfully synthesized at 21 GPa and 1470 K for 4 h
107 (Table 1, Fig. 1). Aqueous fluid was observed when opening the recovered capsules. Crystals of
108 δ-AlOOH, δ-$(Al_{0.953},Fe_{0.047})$OOH and δ-$(Al_{0.878},Fe_{0.122})$OOH were colorless, yellowish green and
109 brown, respectively, and showed uniform extinction under cross-polarized light. The crystals
110 contained a small number of fluid inclusions (Fig.1).

111 The chemical compositions of the δ-$(Al_{0.953},Fe_{0.047})$OOH and δ-$(Al_{0.878},Fe_{0.122})$OOH
112 crystals were nearly homogeneous within each crystal and among different crystals with
113 Fe/(Al+Fe) of 0.0469(8) and 0.122(3) (Table 2). The Fe contents of the crystals were less than
114 those of the starting materials, most likely due to Fe loss to the $Au_{80}Pd_{20}$ capsule at high
115 temperature (Kawamoto and Hirose, 1994) or a low Fe partition coefficient between
116 δ-(Al,Fe)OOH and aqueous fluid. The Mössbauer spectra showed 95-100% $Fe^{3+}/\Sigma Fe$ with
117 hyperfine parameters consistent with octahedral site occupancy (Fig. 2). Oxide weight deficits

were 17.2(6) and 16.6(4) wt% for δ-$(Al_{0.953},Fe_{0.047})OOH$ and δ-$(Al_{0.878},Fe_{0.122})OOH$, respectively. If we assign the oxide weight deficits to H_2O, these are larger than the H_2O contents based on their ideal chemical formulae (14.68 and 14.18%, respectively).

The unit-cell parameters of δ-AlOOH are a = 4.7139(2) Å, b = 4.2263(2) Å, c = 2.8321(2) Å and V = 56.422(6) $Å^3$ (Table 3, Fig. 3). These values are consistent with those of previous studies (Komatsu et al., 2006; Suzuki et al., 2000). The unit-cell parameters of δ-(Al,Fe)OOH increase with Fe/(Al+Fe). The unit-cell volumes of δ-$(Al_{0.953},Fe_{0.047})OOH$ and δ-$(Al_{0.878},Fe_{0.122})OOH$ deviate positively by 0.27 and 0.75%, respectively, from a straight line connecting values for δ-AlOOH (Komatsu et al., 2006; Suzuki et al., 2000) and ε-FeOOH (Suzuki, 2010). The full widths at half maximum of the omega scans of the 110 spots are 0.054-0.064° (Table 1), demonstrating the high quality of the crystals.

IMPLICATIONS

The synthesis conditions of δ-$(Al_{0.953},Fe_{0.047})OOH$ and δ-$(Al_{0.878},Fe_{0.122})OOH$, 21 GPa and 1470 K, are close to those where δ-AlOOH decomposes to Al_2O_3 corundum and aqueous fluid (Sano et al., 2004). The decomposition temperature of δ-(Al,Fe)OOH may not be substantially affected, therefore, by Fe substitution in this phase. The excess volumes of

δ-$(Al_{0.953},Fe_{0.047})OOH$ and δ-$(Al_{0.878},Fe_{0.122})OOH$ (0.27 and 0.75%, respectively) are smaller than those of Fe-bearing corundum in the Al_2O_3-Fe_2O_3 system (e.g., 1.52% for $(Al_{0.909},Fe_{0.091})_2O_3$) (Majzlan et al., 2002). The relatively small excess volume of δ-(Al,Fe)OOH supports Fe substitution up to Fe/(Al+Fe) = 0.122 in this phase. If δ-(Al,Fe)OOH were as stable as δ-AlOOH in terms of pressure-temperature conditions (Sano et al., 2008), δ-(Al,Fe)OOH could play an important role in the cycling of water (hydrogen) and Fe^{3+} (oxygen) in the deep Earth. Further study is necessary to determine the stability of δ-(Al,Fe)OOH.

The single crystals of δ-(Al,Fe)OOH synthesized in this study are ideal for preparation of single-crystal samples with specific dimensions, shape and, if needed, crystallographic orientation. Such samples are particularly well suited for high-pressure experiments using a diamond anvil cell and would enable studies of phase stability, physical properties such as elasticity and elastic anisotropy, behavior of hydrogen bonding and the spin state of Fe. Consequently, single crystals of δ-(Al,Fe)OOH can contribute to the advancement of high-pressure mineralogy.

ACKNOWLEDGMENTS

We are grateful to R. Njul, Y. Ito, and H. Fischer for their support in sample polishing, chemical analysis and manufacturing of cell assembly parts, respectively. We thank A. Shatskiy and two anonymous reviewers for helpful reviews. This study was supported by the International Research Training Group "Deep Earth Volatile Cycles" funded by the German Research Foundation (DFG) and the Japan Society for the Promotion of Science (JSPS) and by the JSPS Japanese-German Graduate Externship.

REFERENCES CITED

Angel, R.J., and Finger, L.W. (2011) SINGLE: A program to control single-crystal diffractometers. Journal of Applied Crystallography, 44, 247-251.

Chenavas, J., Joubert, J.C., Capponi, J.J., and Marezio, M. (1973) Synthese de nouvelles phases denses d'oxyhydroxydes $M^{3+}OOH$ des metaux de la premiere serie de transition, en milieu hydrothermal à tres haute pression. Journal of Solid State Chemistry, 6(1), 1-15.

Gleason, A.E., Jeanloz, R., and Kunz, M. (2008) Pressure-temperature stability studies of FeOOH using X-ray diffraction. American Mineralogist, 93, p. 1882.

Kawamoto, T., and Hirose, K. (1994) Au-Pd sample containers for melting experiments on iron and water bearing systems. European Journal of Mineralogy, 6, 381-385.

Keppler, H., and Frost, D.J. (2005) Introduction to minerals under extreme conditions. In R. Miletich, Ed. Mineral behaviour at extreme conditions, EMU notes in mineralogy, 7, p. 1-30. European Mineralogical Union.

King, H.E., and Finger, L.W. (1979) Diffracted beam crystal centering and its application to high-pressure crystallography. Journal of Applied Crystallography, 12, 374–378.

Komatsu, K., Kuribayashi, T., Sano, A., Ohtani, E., and Kudoh, Y. (2006) Redetermination of the high-pressure modification of AlOOH from single-crystal synchrotron data. Acta Crystallographica Section E, 62(11), i216-i218.

Kudoh, Y., Kuribayashi, T., Suzuki, A., Ohtani, E., and Kamada, T. (2004) Space group and hydrogen sites of δ-AlOOH and implications for a hypothetical high-pressure form of $Mg(OH)_2$. Physics and Chemistry of Minerals, 31(6), 360-364.

Kuribayashi, T., Sano-Furukawa, A., and Nagase, T. (2014) Observation of pressure-induced phase transition of δ-AlOOH by using single-crystal synchrotron X-ray diffraction method. Physics and Chemistry of Minerals, 41(4), 303-312.

Majzlan, J., Navrotsky, A., and Evans, B.J. (2002) Thermodynamics and crystal chemistry of the hematite-corundum solid solution and the $FeAlO_3$ phase. Physics and Chemistry of Minerals, 29(8), 515-526.

Marquardt, H., and Marquardt, K. (2012) Focused ion beam preparation and characterization of single-crystal samples for high-pressure experiments in the diamond-anvil cell. American Mineralogist, 97(2-3), 299-304.

188 Morishima, H., Kato, T., Suto, M., Ohtani, E., Urakawa, S., Utsumi, W., Shimomura, O., and
189 Kikegawa, T. (1994) The phase-boundary between α-Mg_2SiO_4 and β-Mg_2SiO_4
190 determined by in-situ X-ray observation. Science, 265, 1202-1203.
191 Nishihara, Y., and Matsukage, K.N. (2016) Iron-titanium oxyhydroxides as water carriers in the
192 Earth's deep mantle. American Mineralogist, 101, p. 919.
193 Ohira, I., Ohtani, E., Sakai, T., Miyahara, M., Hirao, N., Ohishi, Y., and Nishijima, M. (2014)
194 Stability of a hydrous δ-phase, AlOOH-$MgSiO_2(OH)_2$, and a mechanism for water
195 transport into the base of lower mantle. Earth and Planetary Science Letters, 401, 12-17.
196 Ohtani, E., Litasov, K., Suzuki, A., and Kondo, T. (2001) Stability field of new hydrous phase,
197 δ-AlOOH, with implications for water transport into the deep mantle. Geophysical
198 Research Letters, 28(20), 3991-3993.
199 Prescher, C., McCammon, C., and Dubrovinsky, L. (2012) MossA: a program for analyzing
200 energy-domain Mössbauer spectra from conventional and synchrotron sources. Journal of
201 Applied Crystallography, 45(2), 329-331.
202 Ralph, R.L., and Finger, L.W. (1982) A computer-program for refinement of crystal orientation
203 matrix and lattice-constants from diffractometer data with lattice symmetry constraints.
204 Journal of Applied Crystallography, 15, 537–539.
205 Rapp, R.P., Irifune, T., Shimizu, N., Nishiyama, N., Norman, M.D., and Inoue, T. (2008)
206 Subduction recycling of continental sediments and the origin of geochemically enriched
207 reservoirs in the deep mantle. Earth and Planetary Science Letters, 271(1-4), 14-23.

Rubie, D.C. (1999) Characterising the sample environment in multianvil high-pressure experiments. Phase Transitions, 68(3), 431-451.

Sano, A., Ohtani, E., Kondo, T., Hirao, N., Sakai, T., Sata, N., Ohishi, Y., and Kikegawa, T. (2008) Aluminous hydrous mineral δ-AlOOH as a carrier of hydrogen into the core-mantle boundary. Geophysical Research Letters, 35(3), L03303.

Sano, A., Ohtani, E., Kubo, T., and Funakoshi, K.-i. (2004) In situ X-ray observation of decomposition of hydrous aluminum silicate $AlSiO_3OH$ and aluminum oxide hydroxide δ-AlOOH at high pressure and temperature. Journal of Physics and Chemistry of Solids, 65(8-9), 1547-1554.

Suzuki, A. (2010) High-pressure X-ray diffraction study of ε-FeOOH. Physics and Chemistry of Minerals, 37(3), 153-157.

Suzuki, A., Ohtani, E., and Kamada, T. (2000) A new hydrous phase δ-AlOOH synthesized at 21 GPa and 1000 °C. Physics and Chemistry of Minerals, 27(10), 689-693.

Suzuki, A., Ohtani, E., Morishima, H., Kubo, T., Kanbe, Y., Kondo, T., Okada, T., Terasaki, H., Kato, T., and Kikegawa, T. (2000) In situ determination of the phase boundary between wadsleyite and ringwoodite in Mg_2SiO_4. Geophysical Research Letters, 27(6), 803-806.

Terasaki, H., Ohtani, E., Sakai, T., Kamada, S., Asanuma, H., Shibazaki, Y., Hirao, N., Sata, N., Ohishi, Y., Sakamaki, T., Suzuki, A., and Funakoshi, K.-i. (2012) Stability of Fe-Ni hydride after the reaction between Fe-Ni alloy and hydrous phase (δ-AlOOH) up to 1.2

Mbar: Possibility of Hcontribution to the core density deficit. Physics of The Earth and Planetary Interiors, 194-195, 18-24.

FIGURE CAPTIONS

Figure 1. Photographs of the samples. (**a**) Cross section of the capsule (run H4444). Single crystals of (**b**) δ-AlOOH, (**c**) δ-$(Al_{0.953},Fe_{0.047})$OOH and (**d**) δ-$(Al_{0.878},Fe_{0.122})$OOH. The fluid inclusion is indicated with an arrow in (**b**).

Figure 2. Mössbauer spectrum of δ-$(Al_{0.953},Fe_{0.047})$OOH. The spectrum was fit to two components, each assigned to Fe^{3+} in the octahedral site: a quadrupole doublet (grey with red outline) and a broad magnetic component (blue outline).

Figure 3. Orthorhombic unit-cell parameters of δ-(Al,Fe)OOH. (**a**) *a*. (**b**) *b*. (**c**) *c*. (**d**) *V*. Open squares and diamonds are those of δ-AlOOH reported in Suzuki et al. (2000) and Komatsu et al. (2006), respectively. *V* of ε-FeOOH (Suzuki, 2010) is also plotted as an open circle in (**d**). Dashed lines connect the end-member values.

This is a preprint, the final version is subject to change, of the American Mineralogist (MSA)
Cite as Authors (Year) Title. American Mineralogist, in press.
(DOI will not work until issue is live.) DOI: http://dx.doi.org/10.2138/am-2017-6153

TABLE 1. Experimental conditions and results

Run No.	Starting material	Recovered sample		Max. size	Omega scan for 110
	Fe/(Al+Fe)	Phase[a]	Fe/(Al+Fe)	(mm)	(°, FWHM[b])
H4444	0	δ, fluid - δ, fluid		0.6	0.064
H4473	0.06	0.0469(8) δ, fluid		0.5	0.058
H4468	0.15	0.122(3)		0.4	0.054

Notes: All runs were performed at 21 GPa and 1470 K for 4

h. [a] Abbreviations: δ = δ-(Al,Fe)OOH; fluid = aqueous fluid.

[b] Abbreviation: full width at half maximum.

TABLE 2. Chemical compositions of δ-(Al,Fe)OOH single crystals

Run No./	n[a]	Mass (wt%)				Atomic ratio (O = 2)				
Crystal		Al_2O_3	Fe_2O_3	H_2O[b]	Total	Al	Fe	H[b]	Al+Fe	Fe/(Al+Fe)
H4473										
1	10	76.9(4)	6.05(14)	17.1(5)	100	0.908(9)	0.045(1)	1.14(3)	0.953(9)	0.0472(10)
2	10	76.8(5)	5.90(8)	17.3(5)	100	0.905(9)	0.044(1)	1.15(3)	0.949(9)	0.0462(7)
3	10	76.5(9)	6.12(11)	17.3(10)	100	0.901(17)	0.045(1)	1.16(5)	0.947(18)	0.0480(8)
4	10	77.0(4)	5.94(11)	17.1(5)	100	0.909(8)	0.044(1)	1.14(3)	0.953(9)	0.0463(8)
Average		76.8(5)	6.00(11)	17.2(6)	100	0.906(11)	0.045(1)	1.15(3)	0.951(11)	0.0469(8)
H4468										
1	10	68.3(5)	14.6(3)	17.1(5)	100	0.830(8)	0.111(3)	1.18(3)	0.942(9)	0.118(3)
2	10	67.1(5)	16.3(4)	16.5(7)	100	0.824(10)	0.126(4)	1.15(4)	0.951(13)	0.133(3)
3	10	68.7(3)	15.1(5)	16.1(4)	100	0.843(5)	0.117(5)	1.12(2)	0.960(8)	0.122(4)
4	9	68.6(3)	14.9(3)	16.5(2)	100	0.838(4)	0.115(2)	1.14(1)	0.952(5)	0.120(2)
5	10	69.0(3)	14.5(2)	16.5(4)	100	0.843(6)	0.112(2)	1.14(2)	0.954(8)	0.117(1)
Average		68.4(4)	15.1(3)	16.6(4)	100	0.835(7)	0.116(3)	1.14(3)	0.952(9)	0.122(3)

Notes: Numbers in parentheses are one standard deviation on the last digit.

[a] Number of analyses.

[b] H_2O content was calculated from deficit in total mass.

258

TABLE 3. Unit-cell parameters of δ-(Al,Fe)OOH and ε-FeOOH

Run No./ Reference	Fe/(Al+Fe)	*a* (Å)	*b* (Å)	*c* (Å)	*V* (Å^3)	Method
This study						
H4444	0	4.7139(2)	4.2263(2)	2.8321(2)	56.422(6)	SC-XRD
H4473	0.0469(8)	4.7291(2)	4.2397(2)	2.8421(2)	56.984(5)	SC-XRD
H4468	0.122(3)	4.762(3)	4.262(3)	2.858(3)	58.00(8)	SC-XRD
Previous studies						
Suzuki et al. (2000)	0	4.7134(1)	4.2241(1)	2.83252(8)	56.395(5)	Powder XRD[a]
Komatsu et al. (2006)	0	4.7128(11)	4.2221(15)	2.8315(7)	56.34(3)	SC-XRD
Suzuki (2010)	1	4.954(1)	4.4540(9)	3.0001(8)	66.20 (3)	Powder XRD[b]

[a] The unit-cell parameters were refined by the Rietveld method.

[b] The XRD pattern was taken using synchrotron X-ray by energy-dispersive mode.

259

260

261

262

263

264

Figure 1

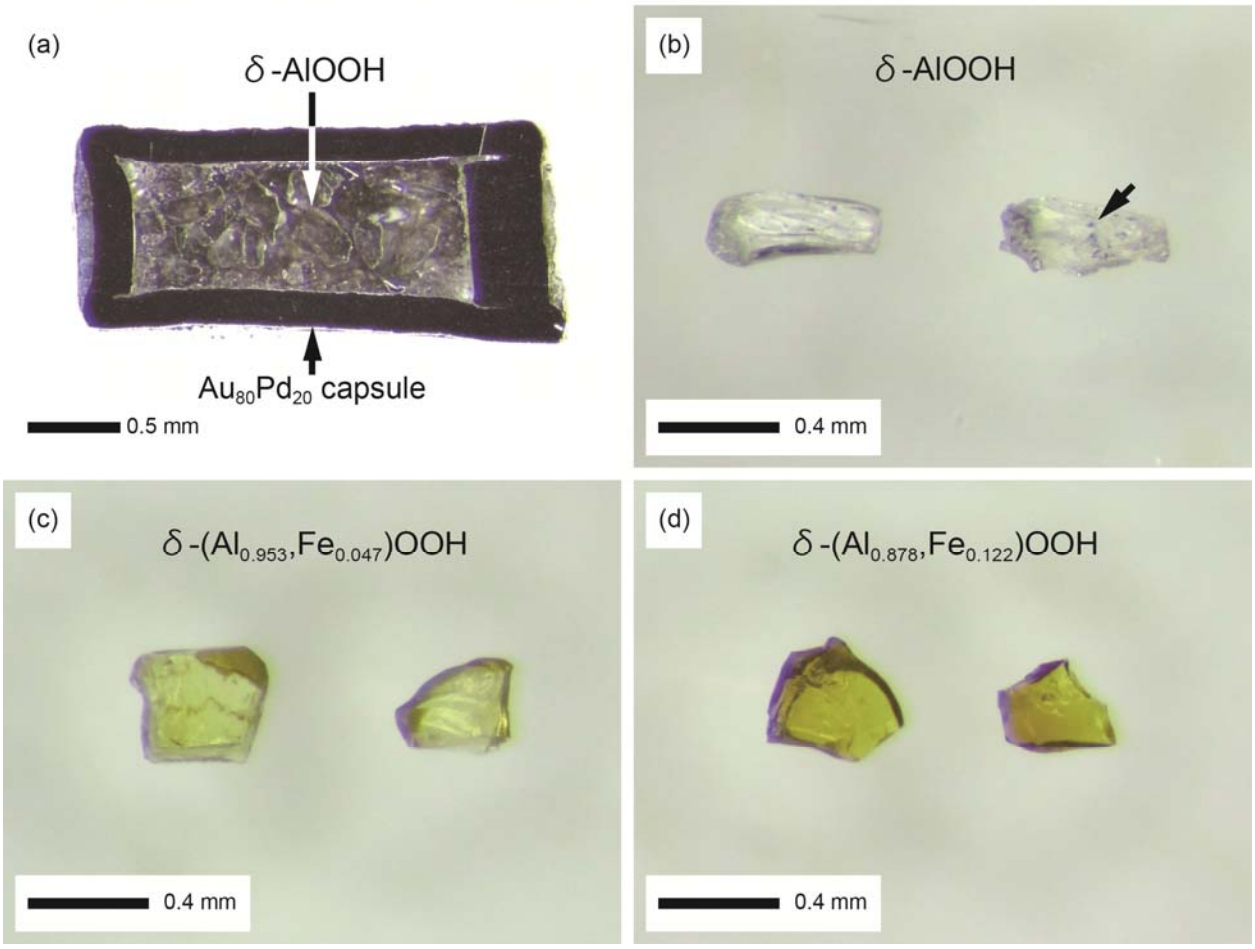

This is a preprint, the final version is subject to change, of the American Mineralogist (MSA)
Cite as Authors (Year) Title. American Mineralogist, in press.
(DOI will not work until issue is live.) DOI: http://dx.doi.org/10.2138/am-2017-6153

Figure 2

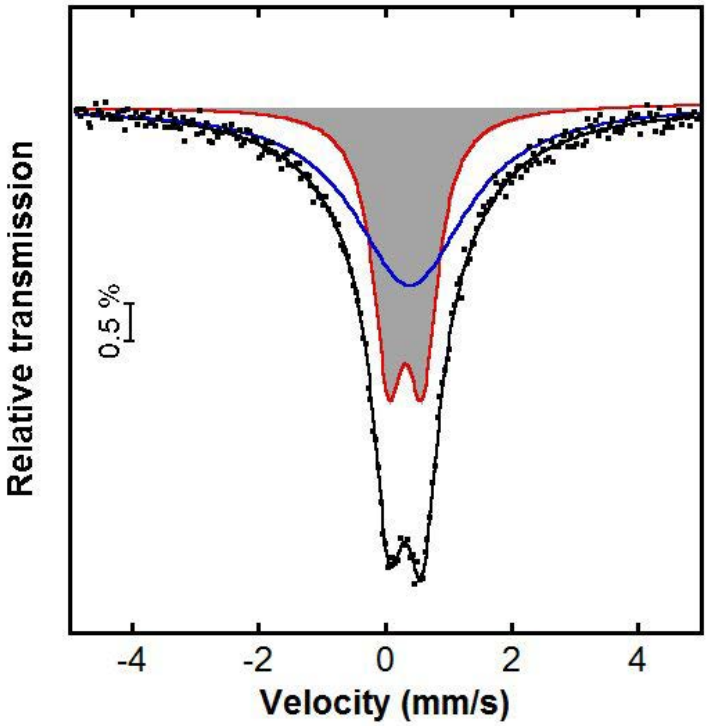

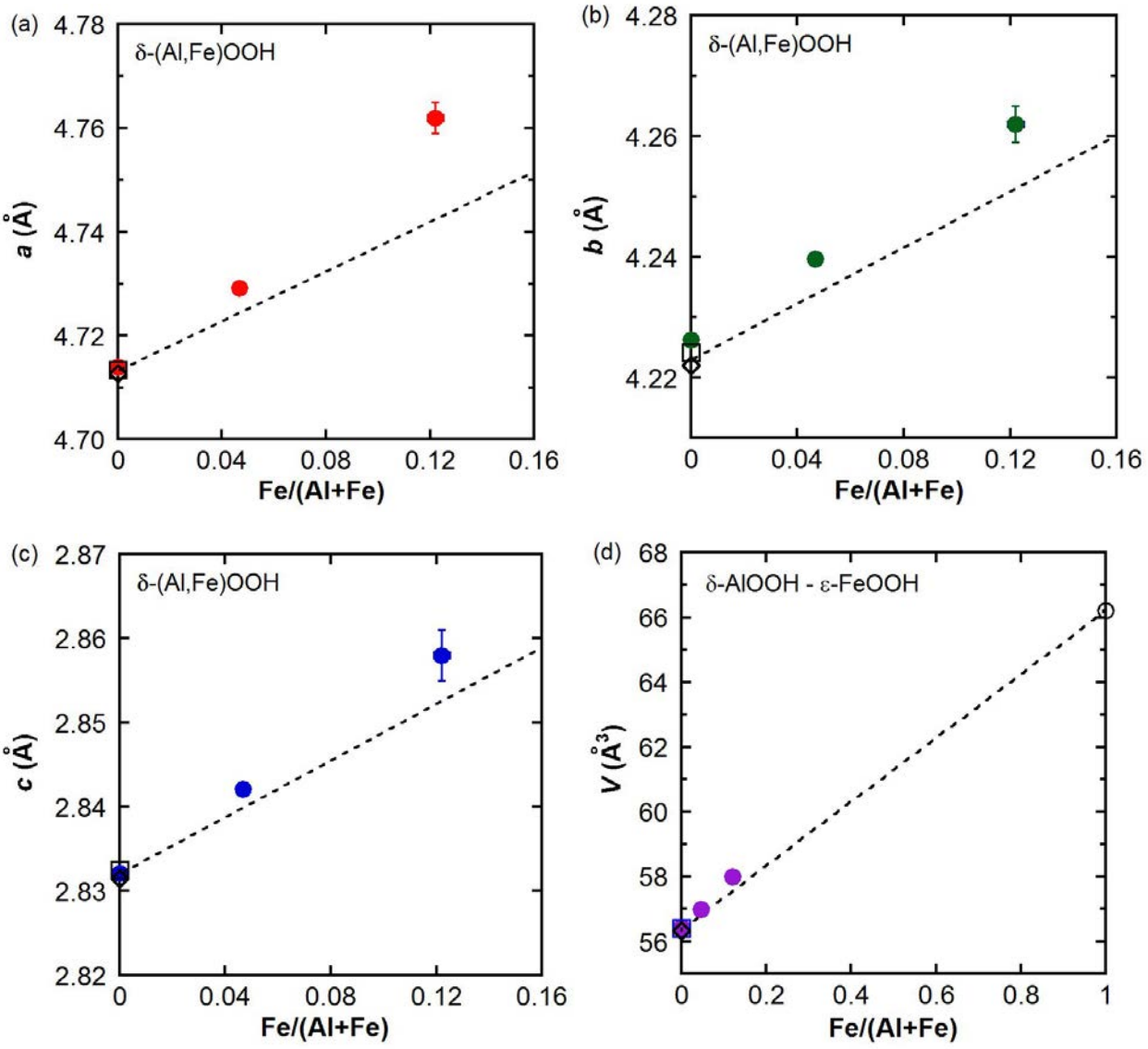

285

286